Supporting Information

Porous Carbon Confined Co_xS_y Nanoparticles Derived from ZIF-67 for Boosting Lithium-Ion Storage

Xiao Su [a], Wen Li [a, *], Haining Sun [b], Jian Wang [b, *], Sisi Hu [a], Fei Yuan [a], Di Zhang [a], Bo Wang [a, *]

[a] Hebei Key Laboratory of Flexible Functional Materials, School of Materials Science and Engineering, Hebei University of Science and Technology, Shijiazhuang 050000, China

[b] Innovation Center for Hebei Intelligent Grid Distribution Technology, Shijiazhuang Kelin Electric Co., Ltd, Shijiazhuang 050000, China

*Corresponding authors.

E-mail addresses: liwen_cc@yeah.net (W. L), wangjian0534@sina.com (J. W), wangbo1996@gmail.com (B. W).

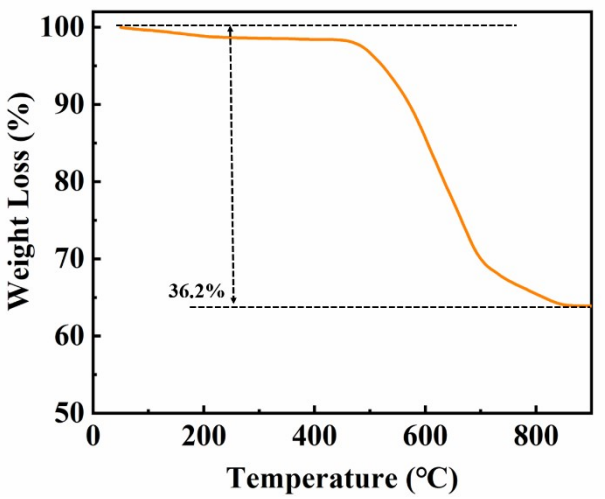

Fig. S1. TGA curve of Co_xS_y powder under nitrogen atmosphere.

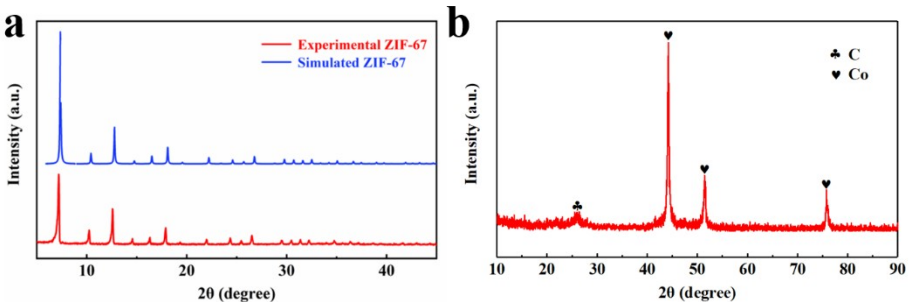

Fig. S2. XRD patterns of ZIF-67 (a) and ZIF-67(600) (b).

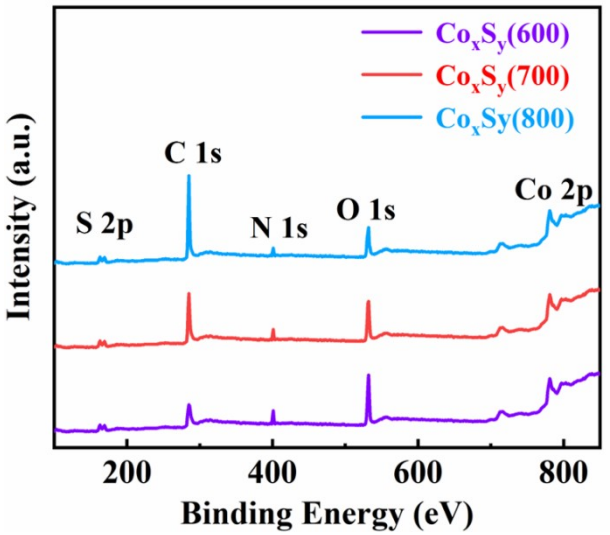

Fig. S3. XPS survey spectrum of Co_xS_y(600), Co_xS_y(700), and Co_xS_y(800).

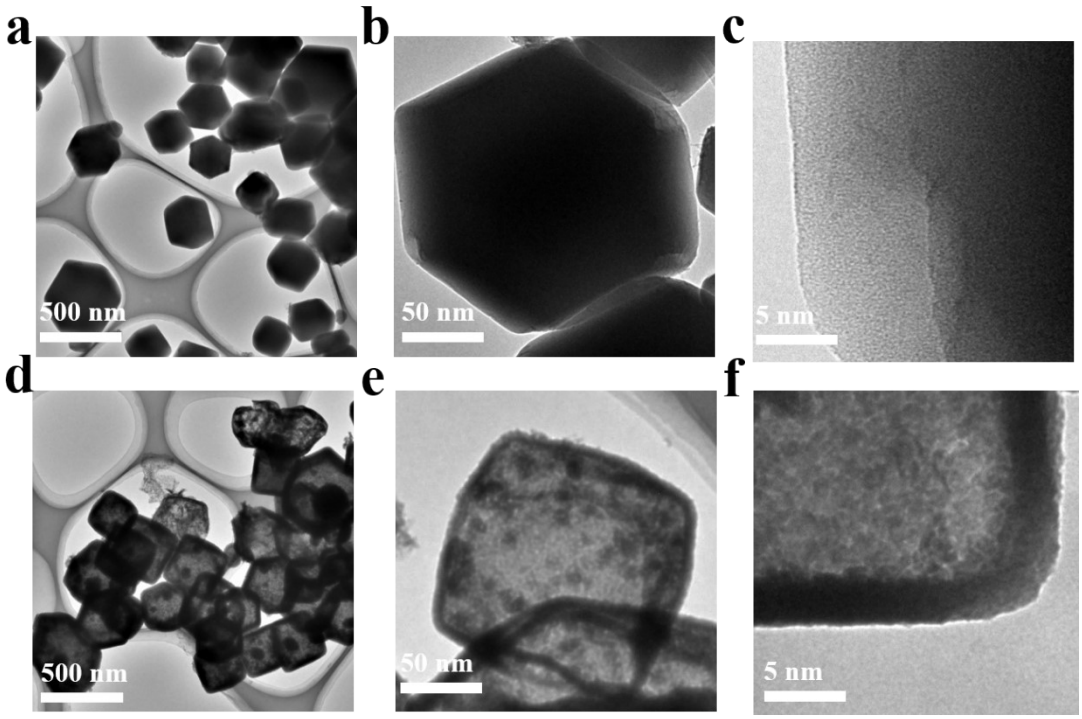

Fig. S4. TEM images of ZIF-67 (a-c) and hollow Co_xS_y (d-f).

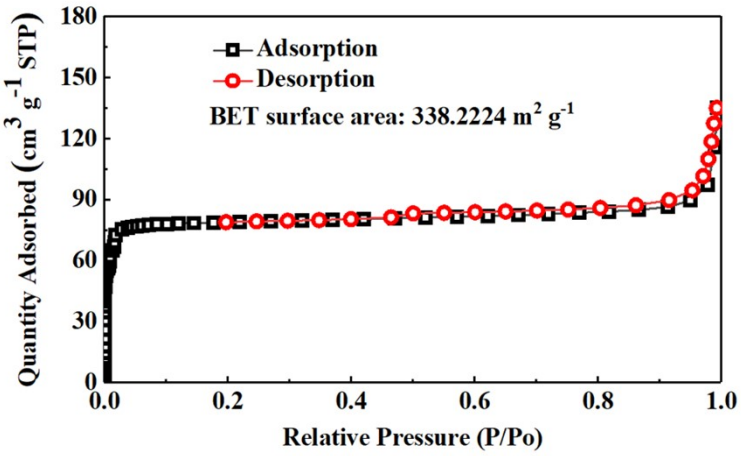

Fig. S5. N_2 adsorption-desorption isotherms of Co_xS_y(700).

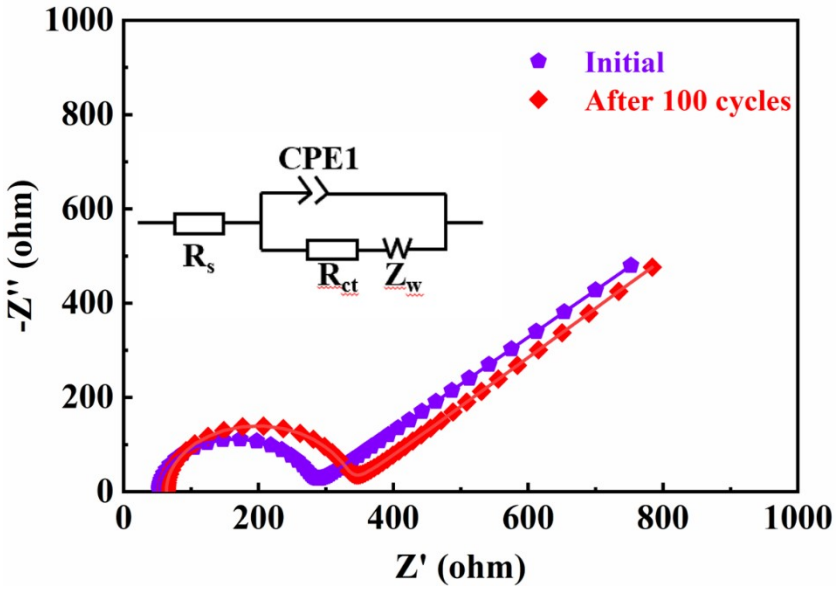

Fig. S6. Electrochemical impedance spectroscopy (EIS) of Co_xS_y(700) at 1 A g^{-1} before and after 100 cycles.

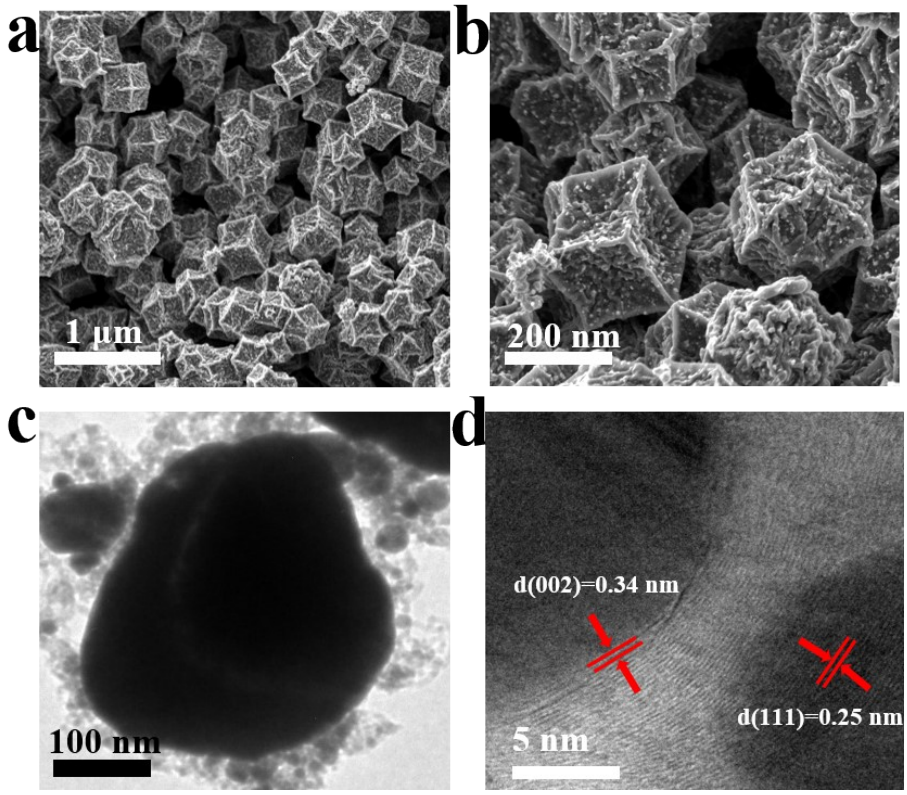

Fig. S7. (a, b) SEM images and (c, d) TEM images of ZIF-67(600).

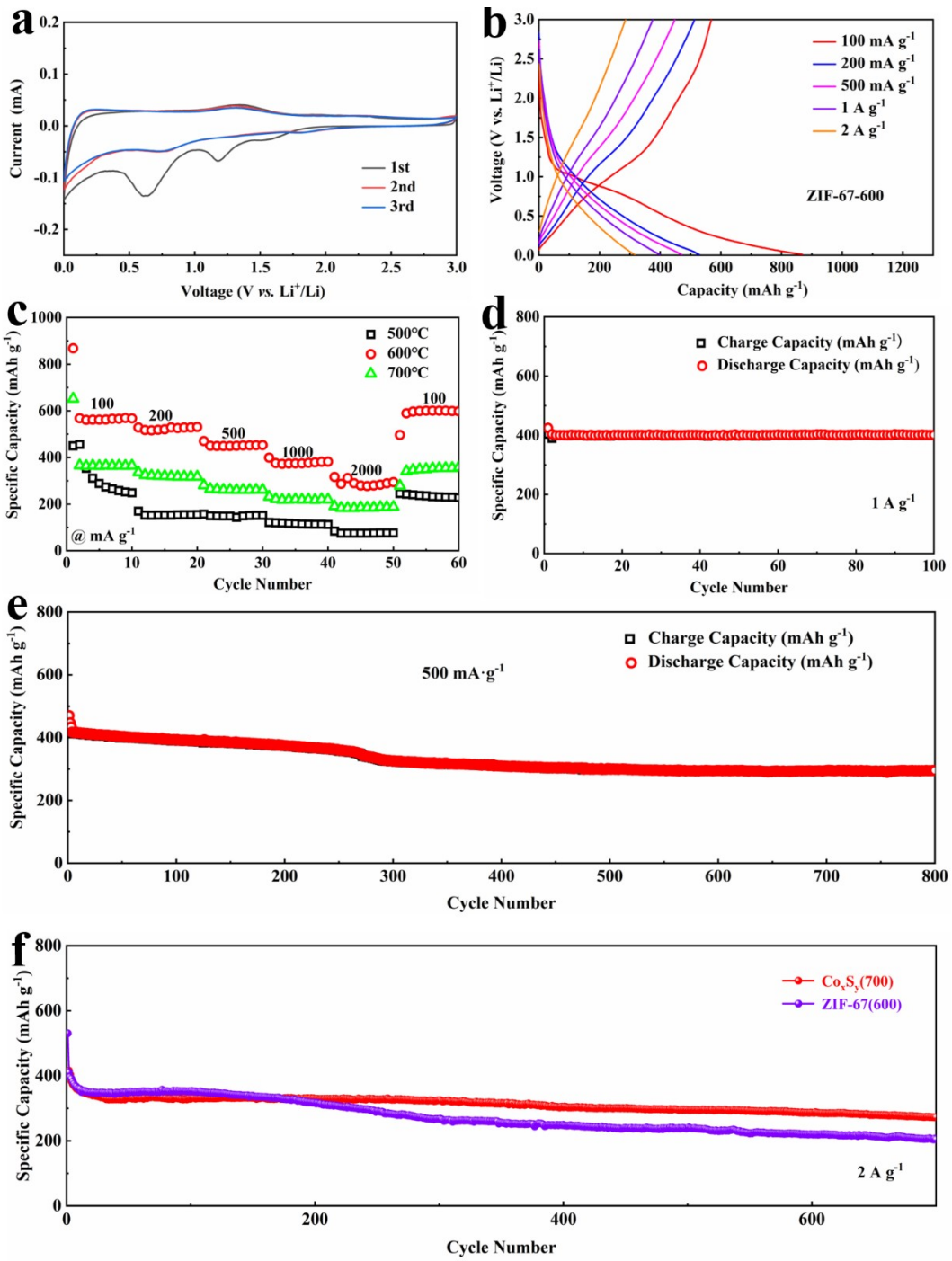

Fig. S8. CV curve (a) and galvanostatic charge-discharge curves at different rates (b) of ZIF-67(600). Rate performance (c) of ZIF-67(*m*); cycling stability at 1 A g^{-1} (d) and 500 mA g^{-1} (e) of ZIF-67(600). (f) The cycling performance comparison of ZIF-67(600) and Co_xS_y(700) at 2 A g^{-1} for 700 cycles.

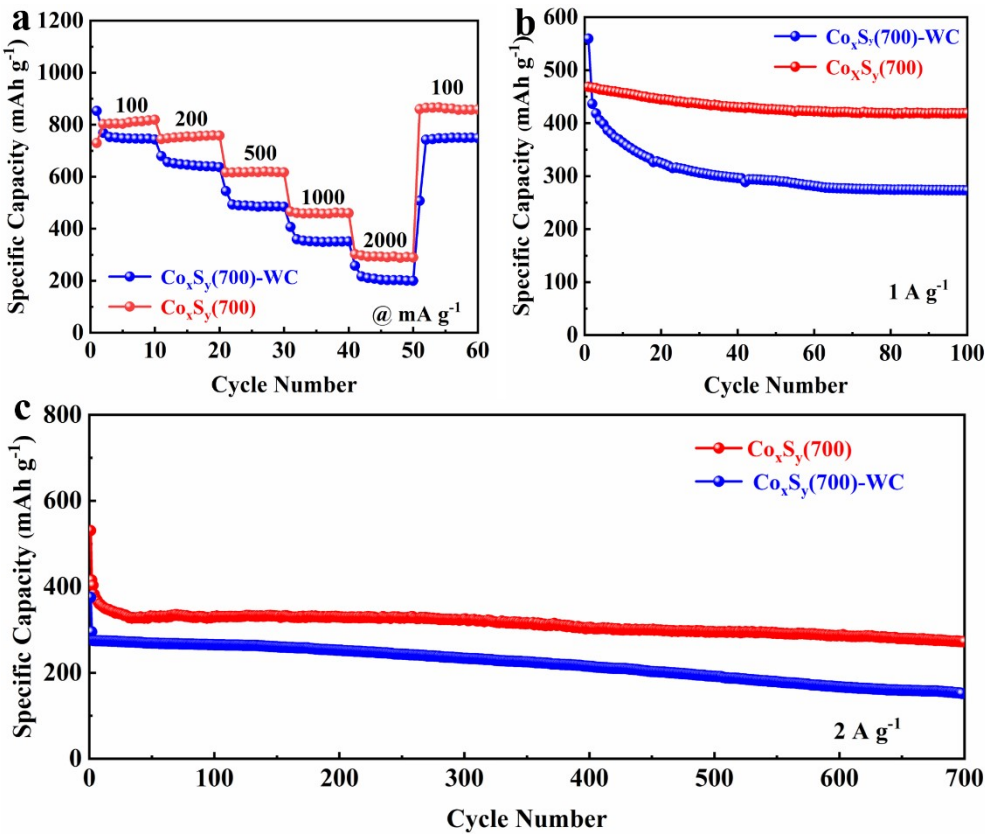

Fig. S9. The comparison of rate (a), cycle (b), and long cycle (c) for $Co_xS_y(700)$ and $Co_xS_y(700)$-WC.